Study of Ruthenium compounds for the photooxidation of alcohols in water

Estudiant: Francesc Rigau Ruvirola

Grau en Química

Correu electrònic: francescrigauruvirola@gmail.com

Tutor: Mª Isabel Romero

Empresa / institució: Universitat de Girona

Vistiplau tutor:

Nom del tutor: Mª Isabel Romero

Empresa / institució: Universitat de Girona

Correu(s) electrònic(s): marisa.romero@udg.edu

ÍNDEX

AGRAÏMENTS

A la doctora Marisa Romero, tutora del treball de fi de grau, per la seva exigència, consells i ajut a la hora de realitzar aquest projecte. També, gràcies als altres estudiants de treball de fi de grau, companys de classe i alhora amics amb els quals he pogut compartir moltes hores i han fet que treballar fos molt menys feixuc tant en la feina pràctica de laboratori, com en la teòrica al despatx.

RESUM

En aquest treball de final de grau s'ha desenvolupat i optimitzat una ruta sintètica per obtenir diferents complexos de ruteni amb lligands tipus N-donors. Posteriorment, s'ha avaluat l'eficiència d'un aqua complex com a catalitzador per a la fotooxidació d'alcohols.

Inicialment, s'ha sintetitzat un dels lligands N-donors no comercial (pypz-pyrene) **L3.** Seguidament, s'ha sintetitzat el producte de partida [RuCl$_3$(trpy)] **C1** el qual, reacciona amb el lligand **L3** per generar una mescla de cloro complexos *cis* i *trans*-[RuCl(trpy)(pypz-pyrene)](PF$_6$) **C2b** i **C2a**. Aquests isòmers han pogut ser separats mitjançant una columna cromatogràfica. Posteriorment a partir del cloro complex **C2a** s'ha sintetitzat l'aqua-complex *trans*-[Ru(trpy)(pypz-pyrene)(OH$_2$)](PF$_6$)$_2$ **C3a**.

Tots el compostos han sigut caracteritzats mitjançant tècniques espectroscòpiques en dissolució (RMN, UV-Visible, ESI-MS) i alguns d'ells mitjançant difracció de Raig X.

Les propietats redox dels compostos han sigut estudiades mitjançant CV i DPV.

S'han pogut funcionalitzar elèctrodes de grafit amb el complex **C2a** i **C3a** mitjançant un procés d'electropolimerització gràcies a la presència del grup pirè. El diagrama de Pourbaix presentat pel compost *trans*-[Ru(trpy)(pypz-pyrene)(OH$_2$)](PF$_6$)$_2$ **C3a** ha permès obtenir informació d'equilibris redox així com extreure els corresponents valors de pKa de les espècies de Ru^{II} i Ru^{III}.

Per acabar, s'ha avaluat l'activitat catalítica del complex *trans*-[Ru(trpy)(pypz-pyrene)(OH$_2$)](PF$_6$)$_2$ **C3a** mitjançant la fotooxidació de 1-fenil etanol en aigua i s'ha observat una moderada conversió amb un excel·lent valor de selectivitat.

RESUMEN

En este Trabajo de final de grado se ha desarrollado y optimizado una ruta sintética para obtener diferentes complejos de rutenio con ligandos tipo N-dadores. Posteriormente, se ha evaluado la eficiencia de un aqua complejo como catalizador para la fotooxidación de alcoholes.

Inicialmente, se ha sintetizado uno de los ligandos N-dadores no comercial (pypz-pyrene) **L3**. Seguidamente, se ha sintetizado el producto de partida [RuCl$_3$(trpy)] **C1** el cualreacciona con el ligando **L3** para generar una mezcla de cloro complejos *cis* i *trans*-[RuCl(trpy)(pypz-pyrene)](PF$_6$) **C2b** i **C2a**. Estos isómeros han podido ser separados mediante una columna cromatográfica. Posteriormente a partir del cloro complejo **C2a** se ha sintetizado el aqua-complejo *trans*-[Ru(trpy)(pypz-pyrene)(OH$_2$)](PF$_6$)$_2$ **C3a**.

Todos los compuestos han sido caracterizados mediante técnicas espectroscópicas en disolución (RMN, UV-Visible, ESI-MS) y algunos de ellos mediante difracción de Rayos X.

Las propiedades redox de los compuestos han sido estudiadas mediante CV i DPV.

Se han podido funcionalizar electrodos de grafito con el complejo **C2a** i **C3a** mediante un proceso de electropolimerización gracias a la presencia del grupo pireno. El diagrama de Pourbaix presentado para el compuesto *trans*-[Ru(trpy)(pypz-pyrene)(OH$_2$)](PF$_6$)$_2$ **C3a** ha permitido obtener información de equilibrios redox así como extraer los correspondientes valores de pKa de las especies de Ru^{II} i Ru^{III}.

Para acabar, se ha evaluado la actividad catalítica del complejo *trans*-[Ru(trpy)(pypz-pyrene)(OH$_2$)](PF$_6$)$_2$ **C3a** mediante la fotooxidación de 1-fenil etanol en agua y se ha observado una moderada conversión con un excelente valor de selectividad.

SUMMARY

In this dissertation work an optimized synthetic route has been developed to obtain different ruthenium complexes with N-donor ligand types. Afterwards, the efficiency of an aqua complex as a catalyst for the photo oxidation of alcohols has been evaluated.

Initially, one of the non-commercial N-donor ligands (pypz-pyrene) **L3** and then the starting product [RuCl$_3$(trpy)] **C1** have been synthetized. This last one reacts with the ligand **L3** to generate a mixture of chloro compounds *cis* and *trans*-[RuCl(trpy)(pypz-pyrene)](PF$_6$) **C2b** and **C2a**. These isomers have been separated by a chromatographic column. Later, starting from the chloro complex **C2a** the aqua-complex *trans*-[Ru(trpy)(pypz-pyrene)(OH$_2$)](PF$_6$)$_2$ **C3a** has been synthetized.

All the compounds have been characterized in solution through spectroscopic techniques (RMN, UV-Visible, ESI-MS) and some of them by X-ray diffraction.

The redox properties of the compounds have been studied by CV and DPV.

It was possible to funcionalize graphite electrodes for the complexes **C2a** and **C3a** by an electro polimerization process thanks to the presence of the pyrene group. The Pourbaix diagram presented for the compound *trans*-[Ru(trpy)(pypz-pyrene)(OH$_2$)](PF$_6$)$_2$ **C3a** has allowed to obtain information of the redox equilibrium as well as extract the correspondent pKa values of the Ru^{II} i Ru^{III}.

Finally, the catalytic activity of the complex *trans*-[Ru(trpy)(pypz-pyrene)(OH$_2$)](PF$_6$)$_2$ **C3a** has been evaluated by the photo oxidation of 1-phenil ethanol in water and it has been observed a moderate conversion with an excellent selectivity value.

GLOSSARY OF TERMS AND ABBREVIATIONS

Abs	Absorbance
acetone-d_6	Deuterated acetone
Anal. Found (Calc.)	Analysis found (analysis calculated)
trpy	2,2';6',2''-terpyridine
Cl	Cloride
$CDCl_3$	Deuterated chloroform
CD_2Cl_2	Deuterated dichloromethane
CV	Cyclic voltammetry
d	Doblet
ε	Extinction coefficient
E	Potential
$E_{1/2}$	Half-wave potential
ESI-MS	Electrospray ionization mass spectrometry
ET	Electron transfer
h	Hours
IR	Infrared
J	Coupling constant
M	Metal
m	Multiplet
MHz	Megahertz
MLCT	Metal to ligand charge transfer
MeOH	Methanol
Methanol-d_4	Deuterated methanol
m/z	Mass-to-charge ratio
NMR	Nuclear magnetic resonance
PCET	Proton-coupled-electron transfer
ppm	Parts per million
pypz-H	2-(3-pyrazolyl)pyridine
pypz-pyrene	2-(1-pyrene-3-pyrazolyl)pyridine
s	Singlet
Ru	Ruthenium
RT	Room Temperature
T	Temperature
t	Triplet
TBAH	Tetra(n-butyl)ammonium hexafluorophosphate
UV-Vis	Ultraviolet-visible spectroscopy
λ	Wavelength
δ	Chemical shift

CHAPTER 1. INTRODUCTION

1.1 Ruthenium complexes properties

Ruthenium is a metal situated in the d group of the periodic table. The electronic configuration of ruthenium ($[Kr]\ 4d^7\ 5s^1$) makes this metal, together with osmium, unique among most of the elements in displaying the widest range of oxidation states in their complexes. The oxidation state of ruthenium takes place from -2 as in $[Ru(CO)_2]^{2+}$ (d^0) to +8 as in RuO_4 (d^{10}). The synthetic versatility and the kinetic stability of ruthenium complexes in different oxidation states make these complexes particularly interesting. Other characteristics of ruthenium's coordination compounds are their high electron transfer capacity,[1] a robust character of their coordination sphere, their redox-active capacity, their easily available high oxidation states and their applications as redox reagents in many different chemical reactions.

Ruthenium complexes have experienced a large boost in the fields of catalysis,[2] photochemistry and photophysics,[3] and more recently in supramolecular[4] and bio-inorganic chemistry.[5]

The properties of ruthenium complexes are certainly correlated with the nature of the ligands coordinated to the central metal ion. Ruthenium complexes with N-donor ligands are studied due to their spectroscopic, photophysical and electrochemical properties.[6] On the other hand, ruthenium complexes with π-conjugate ligands or systems that enable electronic delocalization have shown specific properties in nonlinear optics, magnetism, molecular sensors and liquid crystals.[7] Furthermore, ruthenium complexes with heterocyclic N-donor ligands are the most used due to their interesting spectroscopic, photophysical and electrochemical properties.[8]
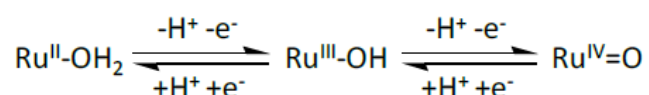
1.2 Ruthenium polypyridyl aqua complexes

In recent years, the study on ruthenium complexes with N-donor ligands have received much attention owing to their interesting uses in diverse areas such as photo sensitizers, as oxidation catalysis[9], for photochemical conversion of solar energy,[10] molecular electronic devices[11] and photoactive DNA cleavage agents for therapeutic purposes.[12]

Extensive coordination chemistry about hexacoordinated complexes containing polypyridyl ligands has been reported, due to the stability of these ligands against oxidation and their great coordinative capacity, increased by their quelating effect. These properties give a great stability to the formed complex.

The redox properties of these complexes become especially interesting when an aqua ligand is directly bonded to the metal center. In this case, a proton-coupled-electron transfer (PCET) is possible, making the high oxidation states fairly accessible.[13]

The successive oxidation from Ru(II) to Ru(IV) are accompanied by a sequential loss of protons favored by the enhanced acidity of the bonded aqua ligand (*Scheme 1*). Therefore, the initial $Ru^{II}\text{-}OH_2$ is oxidized to $Ru^{IV}\text{=}O$, passing through a $Ru^{III}\text{-}OH$ species.

$$Ru^{II}\text{-}OH_2 \underset{+H^+ +e^-}{\overset{-H^+ -e^-}{\rightleftharpoons}} Ru^{III}\text{-}OH \underset{+H^+ +e^-}{\overset{-H^+ -e^-}{\rightleftharpoons}} Ru^{IV}\text{=}O$$

Scheme 1. PCET oxidation process characteristic of Ru-aqua complexes.

1.3 Ruthenium in oxidation catalysis

The development of technologies for the production of chemical fuels or useful compounds with renewable energy (e.g. sunlight) and inexpensive feedstocks relies on an abundant supply of protons and electrons to form the reduced products.
In natural oxygenic photosynthesis, a possible blueprint for artificial photosynthesis, the only suitably abundant source for the needed protons and electrons is water. Oxidation of water liberates protons and electrons and gives off oxygen gas.

The main problem of the water-oxidation reaction is that it is both thermodynamically and kinetically demanding, resulting in slow kinetics without the use of a catalyst.

The first homogeneous water-oxidation catalyst, the ruthenium polypyridyl complex reported by Meyer and co-workers in1982[14], has emphasized the role of proton-coupled electron- transfer (PCET) processes for water activation.

In such processes, oxidation of the metal centre causes a pKa shift of water ligands bound at the metal; the net result is activation of bound water upon metal oxidation, giving hydroxo or oxo complexes upon oxidation of the ruthenium centre.

Enhancing the donor power of the ligand set in each PCET step, by going from aqua to hydroxo to oxo, makes the next oxidation state advance easier to achieve, thus promoting the multielectron oxidation normally considered necessary for water oxidation.[15]

Oxidation of substrates mediated by transition metals is a reaction of great interest from the chemical and biological point of view. In particular, oxidation of olefins, alcohols, amines and sulphides, among others, is interesting from an academic and industrial point of view since the corresponding products play an important role as intermediates and building blocks in synthesis and also in materials science.[16]

For example, epoxides are used in the synthesis of many industrial products, for example, in fine chemical some anti-inflammatory and anti-allergic agents are synthesized from epoxides. Epoxy polymers are widely used in the marine, automotive, aerospace and building industries.

Therefore, one of the challenges of this century is to design catalysts to improve the control of the activity and selectivity of chemical processes and at the same time be compatible and respectful with the environment. Light can be considered an ideal reagent for environmentally friendly, green chemical synthesis; unlike many conventional reagents, visible light is non-toxic, generates no waste and can be obtained from renewable sources. Also, it is an abundant source of energy for driving chemical reactions which is an important pathway toward a sustainable future. Solar energy combined with water is the good alternative energy sources for the development of non-fossil based fuel.[17] Photocatalysts are powerfully enabling in synthetic applications because they absorb light and convert the energy absorbed into chemical potential used to transform organic and inorganic substrat.

During the last decades, a series of homogeneous catalysts were found to be active in this reaction and, among them, we have developed efficient polypyridyl Ru aqua catalysts for chemical oxidation reactions.[18] These Ru aqua complexes can easily lose protons and electrons to form reactive, higher oxidation state Ru=O species, and hence they have been widely used as redox catalysts for the oxidation of both organic and inorganic species. However, few examples of Ru-aqua complexes that can carry out the photoredox transformation of organic substracts have been described in the literature. From the perspective of the sustainability the research and develop of efficient systems is essential to understand a molecular level the reactions involved in the oxidation processes induced by the light.

The oxidation of alcohols is a thermodynamically uphill conversion that involves a two electron-two proton coupled process. [19] This process has a practical importance in the hydrogen-based energy technologies because the anodic liberation of protons and electrons that can be coupled on a cathode for hydrogen fuel production in an integrated photoelectrochemical cell.

$$RCH(\text{-}OH)R' \rightarrow RC(\text{=}O)R' + 2\ H^+ + 2\ e^-$$
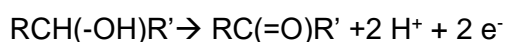
The few studies related to the visible light driven alcohol oxidation have been performed using chromophore/catalyst dyad of ruthenium complexes, [20] one performing as a photosensitizer and the second as a catalyst.

CHAPTER 2. OBJECTIVES

The aims of this work are the ones following:

- To learn the techniques of synthesis and spectroscopic and electrochemical characterization, which are characteristic of a research laboratory.

- The synthesis of a new ligand the pyrz-pyrene and new ruthenium (II) complexes (chloro and aqua), containing polypyridylic ligands such as trpy and pypz-pyrene. The ligands used in this work are the ones following in the Figure 1.
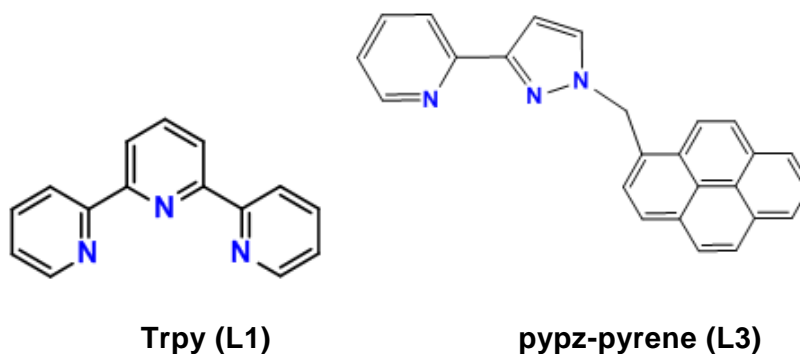

Trpy (L1)   **pypz-pyrene (L3)**

Figure 1. Ligands used in this work

- The spectroscopic and electrochemical characterization of the complexes synthesized.

- Electropolymerization of the complexes onto glassy carbon electrodes.

- Preliminary evaluation of the synthesized aqua-complex in the photooxidation of 1-phenyl ethanol.

CHAPTER 3. EXPERIMENTAL SECTION

3.1 Instrumentation and measurements

- IR

IR spectra were recorded on an Agilent Cary 630 FTIR spectrometer equipped with an ATR MK-II Golden Gate Single Reflection system

- UV-Vis

UV-Vis spectroscopy was performed on a Cary 50 Scan (Varian) UV-Vis spectrophotometer with 1 cm quartz cells.

- Cyclic voltammetry (CV) and differential pulse voltammetry (DPV)

Cyclic voltammetric (CV) and Differential Pulse Voltammetry (DPV) experiments were performed in an IJ-Cambria 660C potentiostat using a three electrode cell. Glassy carbon electrode (3 mm diameter) from BAS was used as working electrode, platinum wire as auxiliary and SCE as the reference electrode. All cyclic voltammograms presented in this work were recorded under nitrogen atmosphere. The complexes were dissolved in solvents containing the necessary amount of $n\text{-Bu}_4N^+PF_6^-$ (TBAH) as supporting electrolyte to yield a 0.1 M ionic strength solution. All $E_{1/2}$ values reported in this work were estimated from cyclic voltammetric experiments as the average of the oxidative and reductive peak potentials ($E_{pa}+E_{pc}$)/2, or directly from DPV. Unless explicitly mentioned the concentration of the complexes was approximately 1mM.

- NMR spectra

The NMR spectroscopy was performed on Bruker DPX 300 and 400 MHz spectrometers. Samples were run in CD_2Cl_2, MeOD, acetone-d_6 or $CDCl_3$. For the NMR assignments, we used the same labeling scheme as for the X-ray structures.

- X-ray Structures Determination

Measurement of the crystals were performed on a Bruker Smart Apex CCD diffractometer using graphite-monochromated Mo Kα radiation (λ = 0.71073Å) from an X-Ray tube.

Data collection, Smart V. 5.631 (BrukerAXS 1997-02); data reduction, Saint+ Version 6.36A (Bruker AXS 2001); absorption correction, SADABS version 2.10 (Bruker AXS 2001) and structure solution and refinement, structure solution and refinement, SHELXL-2013 (Sheldrick, 2013).

- Elemental analyses

Were performed using a CHNS-O Elemental Analyser EA-1108 from Fisons. ESI-MS experiments were performed on a Navigator LC/MS chromatograph from Thermo Quest Finnigan, using acetonitrile as mobile phase.

- ESI-MS experiments

Were performed on a Navigator LC/MS chromatograph from Thermo Quest Finnigan, using methanol as mobile phase.

3.2. Synthesis of compounds

Materials

All reagents used in the present work were obtained from Sigma-Aldrich and were used without further purification. Reagent grade organic solvents were obtained from Carlo Erba and high purity de-ionized water was obtained by passing distilled water through a nano-pure Mili-Q water purification system.

Preparations

2-(3-pyrazolyl)pyridine (pypz-H, **L2**), ligand[21] and [RuCl$_3$(trpy)] (**C1**),[22] complexes were prepared according to literature procedures. All synthetic manipulations were routinely performed under nitrogen atmosphere using Schlenk tubes and vacuum line techniques.

Synthesis of 3-(2-pyridyl)-1-(pyrazolyl)methylpyrene, (pypz-pyrene, L3).

0.06g (2,5mmol) of NaH was washed with hexane under N_2 atmosphere. The washing consisted on adding hexane to the hydride and extracting it with a syringe in order to eliminate the NaH coating. This process was done thrice. Afterwards 0.147g (1mmol) of pypz-H (**L2**) were dissolved in THF anhydrous and added drop by drop over the NaH. The mixture was stirred for 30 minutes at room temperature. Then, 0.3g (1mmol) of 1-(Bromomethyl)-pyrene were added and the mixture was heated at reflux for 35h at 70ºC. A precipitate of NaBr was formed and it was filtered. Then the solution was reduced to the half and pentane was added to precipitate all the remaining salt. The solution was filtered again and dried on a rotary evaporator. A yellow solid corresponding to the ligand appears. **Yield:** 0.264g (73.58 %). **IR (v, cm^{-1}):** 2915, 2874, 1450, 1691, 1350, 1217, 823, 760. **$E_{1/2}$** (CH_2Cl_2 + 0.1M TBAH):1.4 V vs. SCE. **ESI-MS:** [2M+H$^+$]:719. **^{1}H-NMR (400 MHz, CD_2Cl_2):** δ = 6.12 (s, 2H, H9), 6.87 (d, J_{7-8}=2.3Hz, 1H, H7), 7.20 (ddd, J_{2-3}=7.5Hz; J_{2-1}=4.9Hz; J_{2-4}=1.2Hz, 1H, H2), 7.38 (d, J_{8-7}=2.4Hz, 1H, H8), 7.73 (ddd, J_{3-4}=7.9Hz; J_{3-2}=7.5Hz; J_{3-1}=1.8Hz, 1H, H3), 7.89 (d, J_{23-22}=7.8Hz, 1H, H23), 8.02 (m, 1H, H4), 8.06 (d, J_{20-19}=7.6Hz, 1H, H20), 8.11 (m, 2H, H15, H17), 8.19 (d, J_{22-23}=7.9Hz, 1H, H22), 8.23 (m, 3H, H13, H16, H19), 8.36 (d, J_{12-13}= 9.3Hz, 1H, H12), 8.57 (ddd,J_{1-2}=4.9Hz; J_{1-3}=1.8Hz; J_{1-4}=1Hz, 1H, H1).**^{13}C-NMR (400MHz, CD_2Cl_2):** δ = 54.4 (C9), 104.6 (C7), 119.7 (C4), 122.2 (C2), 122.5 (C12), 124.9 (C19), 125.5 (C16), 125.6 (C13), 126.2 (C20), 127.2 (C23), 127.7 (C15, C17), 128.4 (C22), 130.9 (C8), 136.4 (C3), 149.2 (C1).

Synthesis of *trans*- and *cis*-[RuCl(trpy)(pypz-pyrene)](PF$_6$), *trans*-C2a and *cis*-C2b. A sample of **C1** (0.15 g, 0.26 mmol) was added to a 100 mL round bottomed flask containing a solution of LiCl (0.022 g, 0.52 mmol) dissolved in 40 mL of EtOH/H_2O (3:1) under magnetic stirring. Then, NEt$_3$ (0.06 mL, 0.52 mmol) was added and the reaction mixture was stirred at room temperature for 30 min. Afterwards, pypz-pyrene, **L3**, (0.041 g, 0.26 mmol) was added and the mixture was heated at reflux for 3h. The hot solution was then filtered off in a frit and the volume was reduced in a rotary evaporator. After addition of a saturated aqueous solution of NH$_4$PF$_6$ a precipitate formed which was filtered off and washed with water. The solid obtained in this manner was a mixture approximately 1:0.5 of complexes *trans*-**C2a** and *cis*-**C2b**. **Yield:** 139 mg (61%). **Anal. Found (Calc.)** for RuClC$_{40}$N$_6$H$_{28}$PF$_6$·H_2O: C, 54.0 (53.85); H, 3.32 (3.39); N, 9.71 (9.42). **IR (v, cm^{-1}):** 3348, 2935, 2840, 1409, 788. **ESI-MS:** [M-PF$_6$]$^+$ 729.1.

Suitable crystals of complexes were grown as pale yellow plates by diffusion of diethyl ether into a CH_2Cl_2 solution of the brown solid.

For *trans*-**C2a**, **^{1}H-NMR (400 MHz, acetone-d$_6$)**: δ = 5.51 (s, 2H, H9), 5.77 (d, J_{23-22}= 8.0Hz, 1H, H23), 7.33 (d, J_{17-16}=2.7Hz, 1H, H17), 7.36 (d, J_{22-23}=8.04Hz, 1H, H22), 7.42 (ddd, J=7.3Hz; J=5.5Hz; J=1.4Hz, 2H, H27, H39), 7.56 (d, J_{13-12}=9.1Hz, 1H, H12), 7.59 (d, J_{7-8}=2.9Hz, 1H, H7), 7.63 (d, J_{19-20}=8.0Hz, 2H, H19, H20), 7.68 (d, J_{29-28}=J_{37-38}=8.0Hz, 2H, H29, H37), 7.79 (m, 2H, H28, H38), 7.82 (m, 2H, H26, H40), 7.87 (ddd, J_{2-3}=7.4Hz; J_{2-1}=5.7Hz; J_{2-4}=1.5 Hz, 1H, H2), 8.01 (d, J_{13-12}=8.5Hz, 1H, H13), 8.02 (d, J_{8-7}=2.7Hz, 1H, H8), 8.2 (m, 1H, H33), 8.24 (m, 2H, H15, H16), 8.37 (ddd, J_{3-4}=7.8Hz; J_{3-4}=7.5Hz; J_{3-1}=1.6Hz, 1H, H3), 8.43 (d, J_{32-33}=J_{34-33}=7.7Hz, 2H, H32, H34), 8.68 (dt, J_{4-3}=7.8Hz; J_{2-4}=1.2Hz, 1H, H4), 10.15 (dt, J_{1-2}=5.5Hz; J_{1-3}=1.2Hz, 1H, H1). **^{13}C-NMR (400 MHz, acetone- d$_6$)**: δ = 164.1 (C9), 105.7 (C7), 120.6 (C23), 121.2 (C19, C20), 121.5 (C12), 122.3 (C4), 122.7 (C29, C37), 124.4 (C2), 124.8 (C17), 125.8 (C32), 125.9 (C34), 126.6 (C33), 127.1 (C13, C27, C39), 127.8 (C16), 128.5 (C15), 133.1 (C22), 136.3 (C28, C38), 136.8 (C8), 136.9 (C3), 152.2 (C26, C40), 153.2 (C1). **UV-Vis** (CH_2Cl_2) [λ$_{max}$, nm (ε, M^{-1} cm^{-1})]: 327(18656), 346(15351), 407(3827), 502(3821). **$E_{1/2}$** (CH_2Cl_2 + 0.1M TBAH) = 0.85 V vs. SCE.

For *cis*-**C2b**, **^{1}H NMR (400 MHz, Acetone-d$_6$)**: δ = 6.94 (ddd, J_{2-3}=7.4Hz; J_{2-1}=5.9Hz; J_{2-4}=1.5Hz, 1H, H2) 7.42 (m, 3H, H1, H9A, H9B), 7.49 (ddd, J_{27-26}=J_{39-40}=7.6Hz; J_{27-28}=J_{39-38}=5.4Hz; J_{27-29}=J_{39-37}=1.3Hz, 2H, H27, H39), 7.54 (d, J_{12-13}=2.9Hz, 1H, H12), 7.61 (dd, J_{15-16}=5.7Hz; J_{17-16}=3.3Hz, 2H, H15, H17), 7.71 (dd, J_{16-15}=5.7Hz; J_{16-17}=3.2Hz, 1H, H16), 7.69 (m, 1H, H3), 8.00 (m, 2H, H28, H38), 8.05 (d, J_{20-19}=7.6Hz, 1H, H20), 8.08 (m, 1H, H4), 8.11 (d, J_{13-12}=3.1Hz, 1H, H13), 8.16 (m, 3H, H33, H26, H40), 8.23 (d, J_{8-7}=8.9Hz, 1H, H8), 8.26 (d, J_{22-23}=6.8Hz, 1H, H22), 8.30 (d, J_{19-20}=7.6Hz, 1H, H19), 8.36 (d, J_{23-22}=6.9Hz, 1H, H23), 8.58 (dt, J_{29-28}=J_{37-38}=8.1Hz; J_{29-27}=J_{37-39}=1.2Hz, 2H, H29, H37), 8.64 (d, J_{7-8}=9.3Hz, 1H, H7), 8.67 (d, J_{34-33}=J_{32-33}=8.1Hz, 2H, H32, H34). **^{13}C-NMR (400 MHz, acetone- d$_6$)**: δ = 54.0 (C9), 106.0 (C12), 121.9 (C33), 122.5 (C32, C34), 123.4 (C7), 123.6 (C29, C37), 124.3 (C2), 125.1 (C23), 125.6 (C22), 125.8 (C19), 126.4 (C20), 127.4 (C27, C39), 127.8 (C8), 128.0 (C16), 128.4 (C4), 131.1 (C17, C15), 135.8 (C3), 135.9 (C13), 137.1 (C28, C38), 151.7 (C1), 153.7 (C26, C40). **UV-Vis** (CH_2Cl_2) [λ$_{max}$, nm (ε, M^{-1} cm^{-1})]: 325(19142), 344(15245), 407(3832), 503(3785). **$E_{1/2}$** (CH_2Cl_2 + 0.1M TBAH) = 0.88 V vs. SCE.

Synthesis of *trans*-[Ru(trpy)(pypz-pyrene)(OH$_2$)](PF$_6$)$_2$, trans-C3a. A sample of 0.073 g of AgPF$_6$ (0.29 mmol) and 0.1273g of *trans*-**C2a** (0.15 mmol) were added to a solution of 50 ml of a mixture H$_2$O/acetone (2:1), the resulting solution was heated at reflux for 4h in the absence of light. Then, the AgCl formed was filtered off through celite. Afterwards, a saturated aqueous solution of NH$_4$PF$_6$ (1.3 mL) was added to the filtrate and the volume reduced until a precipitate that corresponded to the **C3a** aqua complex was formed. The precipitate formed was filtered through a frit, washed with cold water and diethyl ether and dried at vacuum. The solid obtained in this manner was the aqua complex *trans*-**C3a**. **Yield:** 124.2 mg (85%). **Anal. Found (Calc.)** for RuC$_{40}$N$_6$H$_{30}$OP$_2$F$_{12}$: C, 46.92 (47.06); H, 3.28 (3.02); N, 8.0 (8.39). **IR (v, cm^{-1}):** 3350, 2911, 2863, 1457, 1269, 792, 750.

For *trans*-**C3a**, **1H NMR (400 MHz, Methanol-d4):** δ = 5.42 (s, 2H, H9), 5.65 (d, J$_{23-22}$= 7.8Hz, 1H), 7.28 (d, J$_{22-23}$=7.7Hz, 1H, H22), 7.48 (m, 3H, H17, H27, H39), 7.55 (m, 2H, H12, H7), 7.66 (m, 4H, H19, H20, H29, H37), 7.77 (m, 2H, H28, H38), 7.82 (m, 1H, H2), 7.87 (m, 2H, H26, H40), 7.965 (m, 2H, H8, H13), 8.22(m, 3H, H33, H15, H16), 8.42 (m, 3H, H3, H32, H34), 8,67 (d, J$_{4-3}$=7.8Hz, 1H, H4), 9.38 (d, J$_{1-2}$=5.6Hz, 1H, H1). **UV-Vis** (phosphate buffer pH=6.8) [λ$_{max}$, nm (ε, M^{-1} cm^{-1})]: 334(18976), 345(15351), 393(3731), 467(3836). ***E*$_{1/2}$ (III/I)** and ***E*$_{1/2}$ (IV/II)**, phosphate buffer pH = 6.8: 0.43 V and 0.62V vs. SCE.

3.3. Ethical and sustainability criteria

Due to the experimental processes carried out in a synthetic laboratory, sometimes large quantities of solvent were needed, especially in purification processes like a chromatographic column. However, the residues generated were stored properly, in its respective containers. Also, working maximizing the atomic economy was always a priority. Nevertheless, it has sometimes been difficult to respect because many reactions gave by-products and, as said before, big quantities of solvent were used.
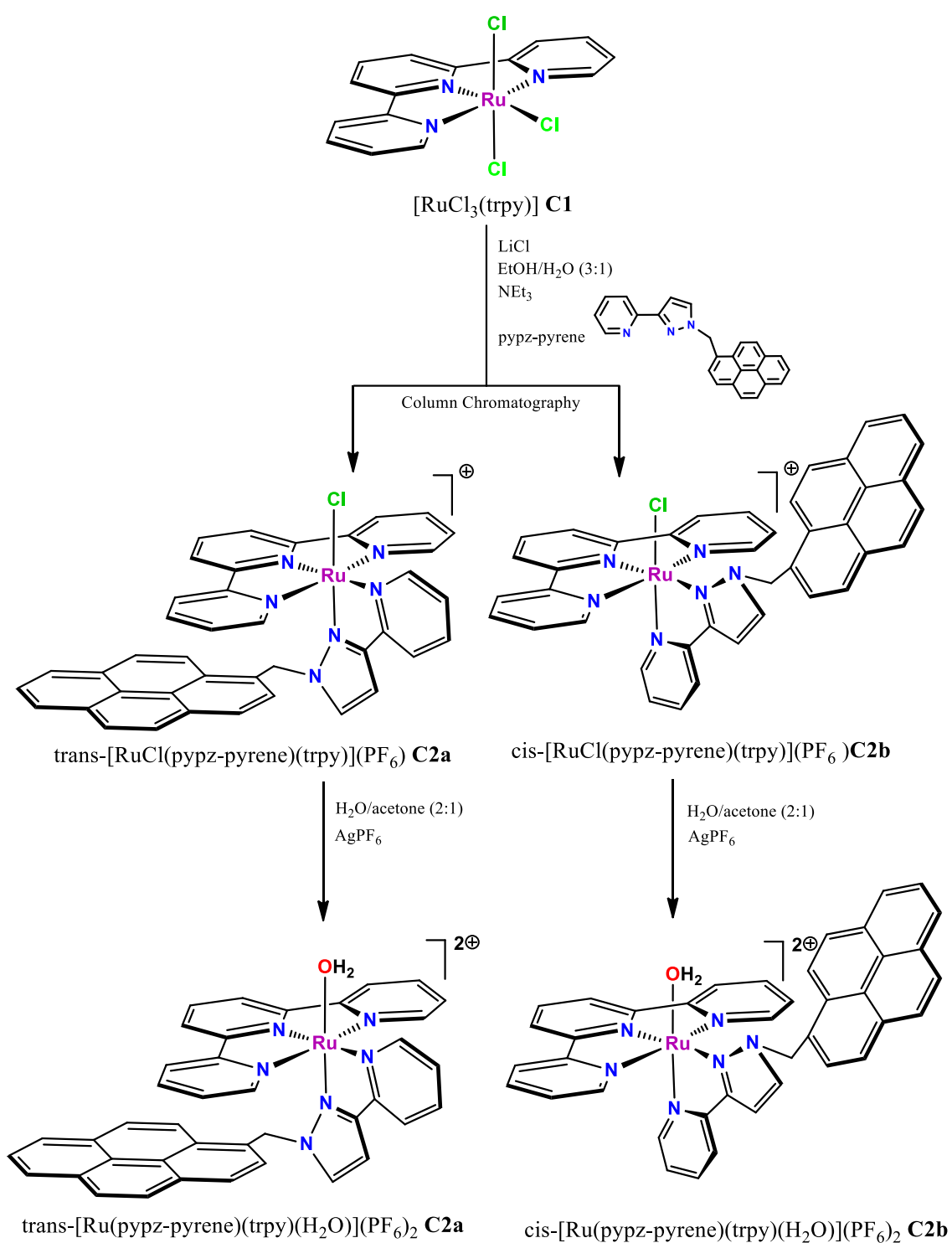
Having said that, however, it is worth mentioning that the purpose of the catalytic study in this work is to reduce the thermal energy needed for a specific reaction, in this case an alcohol oxidation. So, ultimately, the use of this catalyst will help tremendously on keeping the environment cleaner by making the reaction faster and more economical.

CHAPTER 4. RESULTS AND DISCUSSION

4.1 Synthesis and structural characterization of ligand an complexes

The ligand 3-(2-pyridyl)-1-(pyrazolyl)methylpyrene, (pypz-pyrene, **L3**) was obtained by alkylation of the pyrazolic ligand 2-(3-pyrazolyl)pyridine (pypz-H, **L2**) after the addition of 1-(bromomethyl)-pyrene. The synthetic strategy followed for the preparation of Ru^{II} complexes **C2** and **C3**, containing the *trpy* and *pypz-pyrene* ligands, is outlined in Scheme 2. Reaction of equimolar amounts of [RuCl$_3$(trpy)] **C1** and the ligand *pypz-pyrene* in in EtOH:H$_2$O (9:1) in the presence of Et$_3$N (1.2 equivalents) resulted in the substitution of two chlorido ligands in **C1** to generate a 1:0.5 mixture of *trans*-**C2a** and *cis*-**C2b** isomers, after the addition of a saturated NH$_4$PF$_6$ aqueous solution the corresponding chlorido complex **C2.** The formation of two isomers is due to the no symmetric nature of the pypz-pyrene ligand and the nomenclature *cis*- or *trans*- refers to the relative position of the monodentate ligand, Cl or H$_2$O, with regard to the pyrazole ring of the pypz-pyrene ligand. (see Scheme 2). These Ru-Cl complexes are successful separated by chromatographic column, although only a small amount of the *cis* isomer could be obtained pure.

The corresponding *trans*-Ru-OH$_2$ complex **C3a** is easily obtained from the corresponding Ru-Cl, **C2a** complex in the presence AgPF$_6$ in a mixture water/acetone (2:1) after 4 hours hour of reflux.

[RuCl$_3$(trpy)] **C1**

LiCl
EtOH/H$_2$O (3:1)
NEt$_3$

pypz-pyrene

Column Chromatography

trans-[RuCl(pypz-pyrene)(trpy)](PF$_6$) **C2a**

cis-[RuCl(pypz-pyrene)(trpy)](PF$_6$)**C2b**

H$_2$O/acetone (2:1)
AgPF$_6$

H$_2$O/acetone (2:1)
AgPF$_6$

trans-[Ru(pypz-pyrene)(trpy)(H$_2$O)](PF$_6$)$_2$ **C2a**

cis-[Ru(pypz-pyrene)(trpy)(H$_2$O)](PF$_6$)$_2$ **C2b**

Scheme 2. Ligands used in this work and synthetic strategy for the preparation of complexes.

Crystal structures of *trans-* and *cis-***C2a** and **C2b** have been solved by X-ray diffraction analysis. Figures 2 and 3 display their molecular structure whereas the main crystallographic data and selected bond distances and angles can be found in Tables 1 2 and 3.

In all cases, the Ru metal center adopts an octahedrally distorted type of coordination where the trpy ligand is bonded in a meridional manner and the *pypz-pyrene* ligand acts in a bidentate fashion. The sixth coordination site is occupied by the chlorido ligand. All bond distances and angles are within the expected values for this type of complexes[23]. It's worth mentioning the presence of hydrogen bond interactions in both isomers, in the case of *trans-***C2a** between the chlorido ligand and the H1 proton onto the pyridyl ring (2.679 Å) and in the case of *cis-***C2b** the hydrogen bond is observed between one of the methylene protons H9B and the chlorido ligand (2.494 Å).
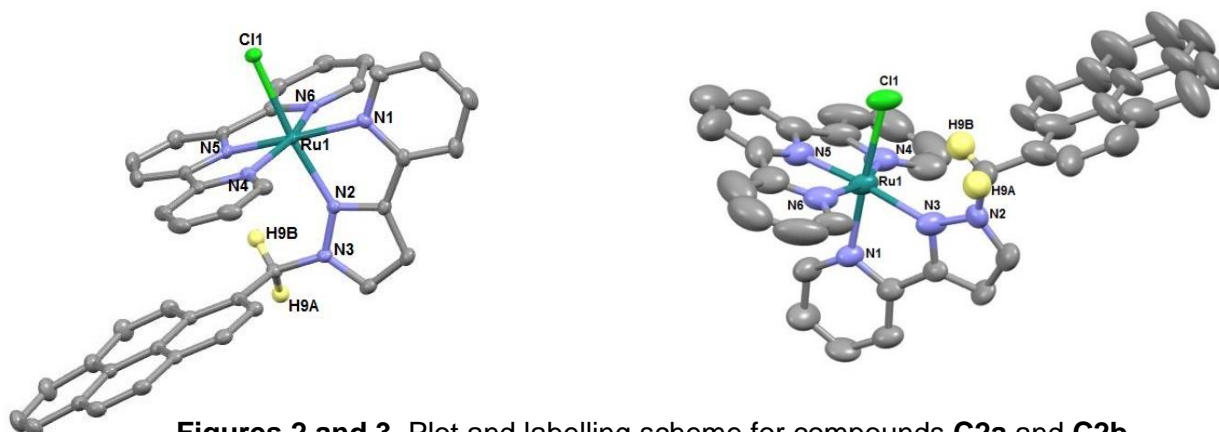
Figures 2 and 3. Plot and labelling scheme for compounds **C2a** and **C2b**

Table 1. Selected bond lengths (Å) and angles (º) for compounds **C2a** and **C2b.**

	*trans-***C2a**	*cis-***C2b**		*trans-***C2a**	*cis-***C2b**
Ru(1)-N(1)	2.099(3)	2.065(8)	**N(2)-Ru(1)-N(6)**	94.17(11)	100.5(4)
Ru(1)-N(2)	2.056(3)	2.110(9)	**N(2)-Ru(1)-N(4)**	90.31(11)	99.8(3)
Ru(1)-N(4)	2.069(3)	2.039(6)	**N(5)-Ru(1)-N(1)**	174.96(11)	96.9(3)
Ru(1)-N(5)	1.954(3)	1.923(5)	**N(6)-Ru(1)-N(1)**	94.61(11)	93.6(3)
Ru(1)-N(6)	2.063(3)	2.063(9)	**N(5)-Ru(1)-Cl(1)**	86.31(8)	85.4(2)
Ru(1)-Cl(1)	2.3969(12)	2.417(3)	**N(6)-Ru(1)-Cl(1)**	89.78(8)	89.6(2)
N(5)-Ru(1)-N(2)	103.02(11)	174.3(3)	**N(1)-Ru(1)-Cl(1)**	93.82(8)	176.3(2)

Table 2. Selected bond lengths (Å) and angles (º) for compounds **C2a** and **C2b.**

	trans-**C2a**	*cis*-**C2b**
N(5)-Ru(1)-N(6)	80.35(12)	79.6(3)
N(5)-Ru(1)-N(4)	79.63(12)	79.9(3)
N(6)-Ru(1)-N(4)	159.99(11)	159.5(3)
N(2)-Ru(1)-N(1)	77.11(11)	77.5(3)
N(4)-Ru(1)-N(1)	105.40(12)	88.1(3)
N(2)-Ru(1)-Cl(1)	170.35(8)	100.3(2)
N(4)-Ru(1)-Cl(1)	88.95(8)	89.5(2)

Table 3. Crystallographic data and details of the structure solution and refinement procedures for the X-ray diffraction of the compounds **C2a** and **C2b.**

	trans-C**2a**	*cis*-C**2b**
Empirical formula	$C_{167}H_{126}Cl_{18}F_{24}N_{24}P_4Ru_4$	$C_{40}H_{28}ClF_6N_6PRu$
Formula weight	4091.17 g/mol	874.17 g/mol
Crystal system	monoclinic	tetragonal
Space group	P 1 21/n 1	P 4/n n c
a[Å]	15.550(9)	17.9714(15)
b[Å]	16.801(7)	17.9714(15)
c[Å]	16.104(8)	49.745(9)
α[º]	90	90
β[º]	103.032(19)	90
γ[º]	90	90
V [Å^3]	4099.(3)	16066.(4)
Formula Units/ cell	1	16
Temp. [K]	100(2)	100(2)
ρ_{calc}, [g/cm^{-3}]	1.657	1.446
μ[mm^{-1}]	0.783	0.561
Final R indices, [I>2σ(I)]	$R_1 = 0.0542$ $wR_2 = 0.1274$	$R_1 = 0.1125$ $wR_2 = 0.2311$
R indices [all data]	$R_1 = 0.0632$ $wR_2 = 0.1369$	$R_1 = 0.1334$ $wR_2 = 0.2469$

4.2 Spectroscopic properties

4.2.1 IR spectroscopy

Figures 4, 5 and 6 show the IR spectra corresponding to the ligand **L3**, the complexes **C2a**, and **C3a**, respectively. The peaks around 3090 cm^{-1}, can be assigned to the ν(=C-H) stretching modes of the polypyridylic ligands. The ones appearing between 1412-1389 cm^{-1}, can correspond to ν(C=N) stretching of the ligands. The peaks observed over 1300-1000 cm^{-1} and at around 830 cm^{-1} correlate to the δ(=C-H) in plane bends. Moreover, all specters show a peak around 845 cm^{-1} that can be assigned to the anion PF_6^-.

Additionally, the aqua complex spectrum displays another peak over 3350 cm-1 which corresponds to the υ(O-H) stretching of the aqua ligand.
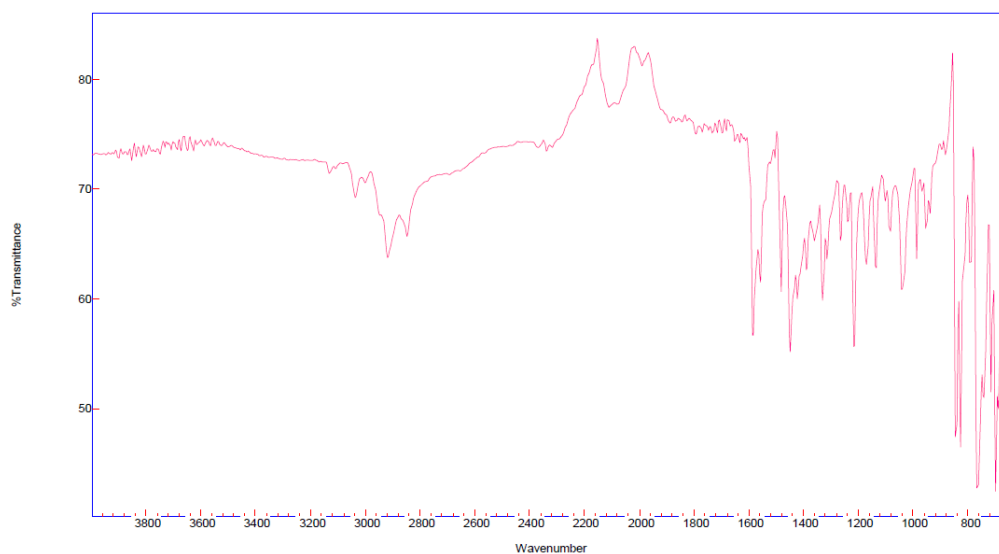
Figure 4. IR spectra of the ligand **L3**

15
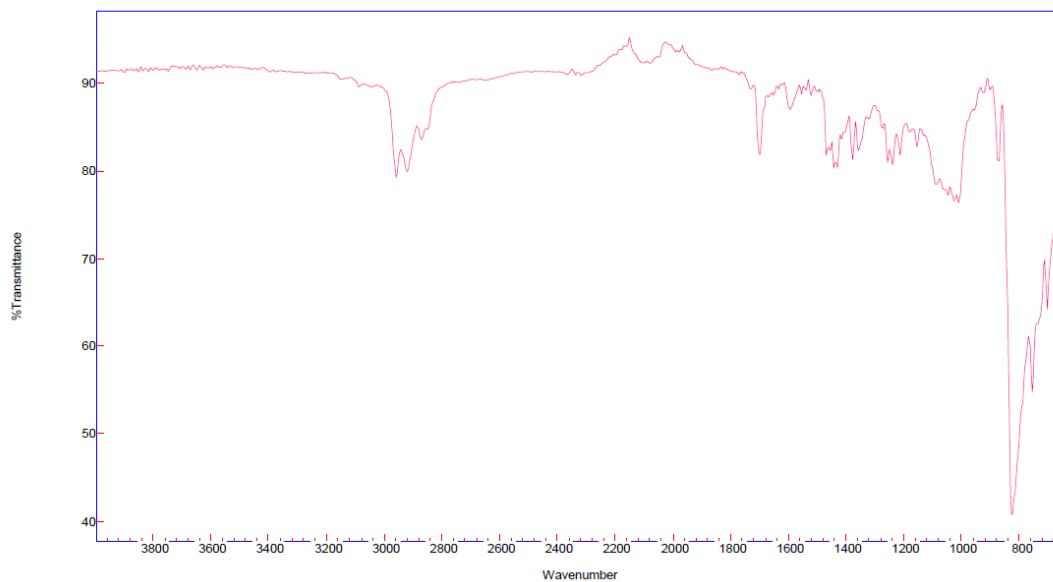
Figure 5. IR spectra of complex **C2a**
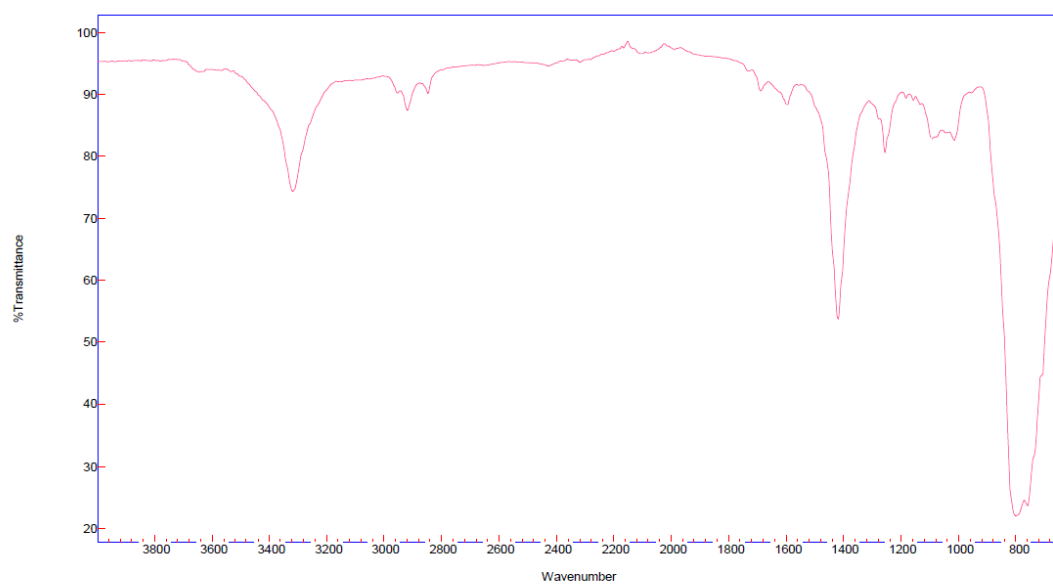
Figure 6. IR spectra of complex **C3a**

4.2.2 NMR spectroscopy

The one-dimensional (1D) and two-dimensional (2D) NMR spectra of ligand pypz-pyrene **L3** and complexes **C2a, C2b** and **C3a** were registered in CD_2Cl_2, acetone-d_6 (for the **C2** complexes) and methanol-d_4, respectively. Figure 7 and 8, show the ^{1}H-NMR and the ^{13}C-NMR spectra of the ligand and Figure 9 and 10 display the ^{1}H-NMR of the isomers **C2a** and **C2b**. The resonances found for the complexes are consistent with the structures obtained in the solid state for both isomers**.** All the resonances for the complexes are found in the aromatic region and have been identified through the COSY and NOESY spectra (not shown).

The most interesting feature of the spectra of chlorido-complexes *trans* and *cis* (Figures 9 and 10) is the deshielding effect exerted by the chlorido ligand over the pyridilic H(1) of the bidentate ligand in the *trans* isomer **C2a** (δ = 10.15 ppm) with regard to cis isomer **C2b** (δ = 7.5 ppm). In the later the H1 is influenced by the aromatic π electron density then appearing upfield with regard to the *trans* isomer a similar effect is observed for the pyrene hydrogens in the trans isomer that are shifted to upfield with respect to those in the cis isomer. It is also worth, mentioning the resonances corresponding to the methylene protons in the pyrene substituent, that in both isomers appear as singlets, which evidence a similar magnetic environment for the two H9 atoms.

In the case of *trans* Ru-OH$_2$ complex the de-shielding effect of the H$_2$O ligand over H(1) is not as strong as that observed in the corresponding chlorido complex *trans*-**C2a**, thus leading to a lower chemical shift (δ = 9.4 ppm) on the **C3a** aqua complex.
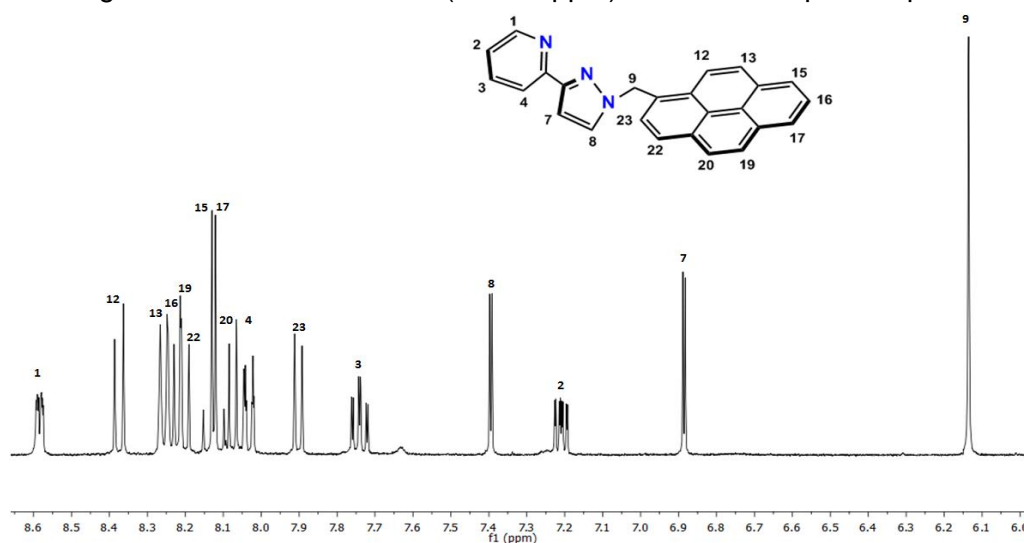

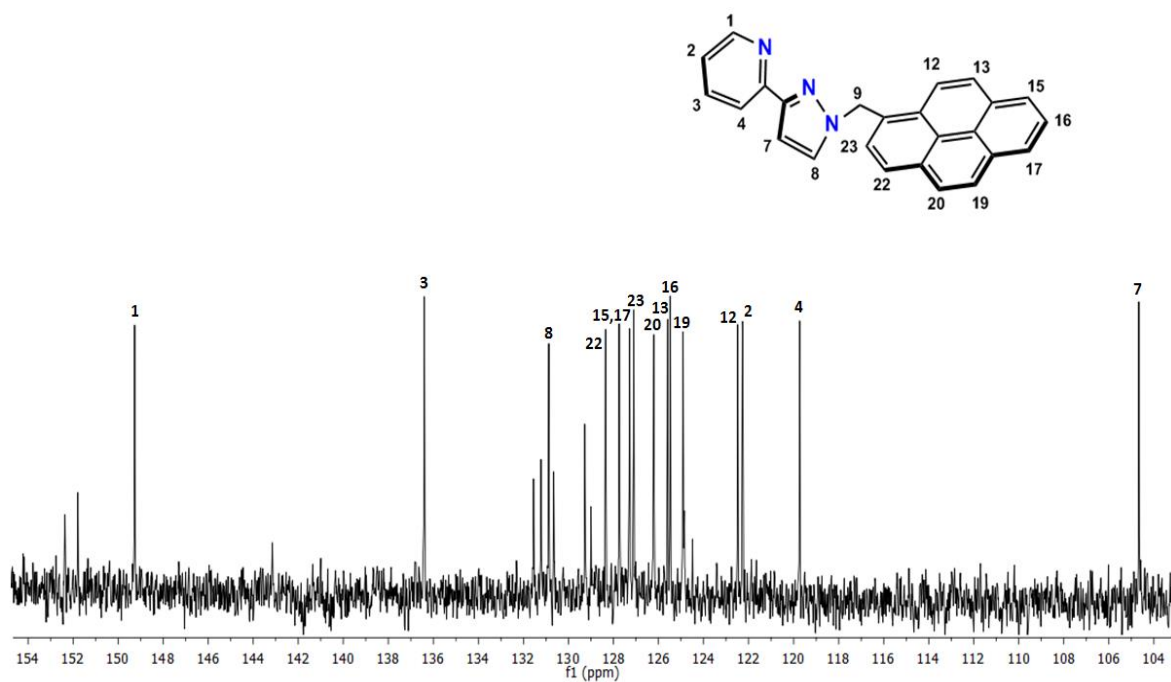**Figure 7**. ^{1}H-NMR spectra corresponding to the ligand **L3**

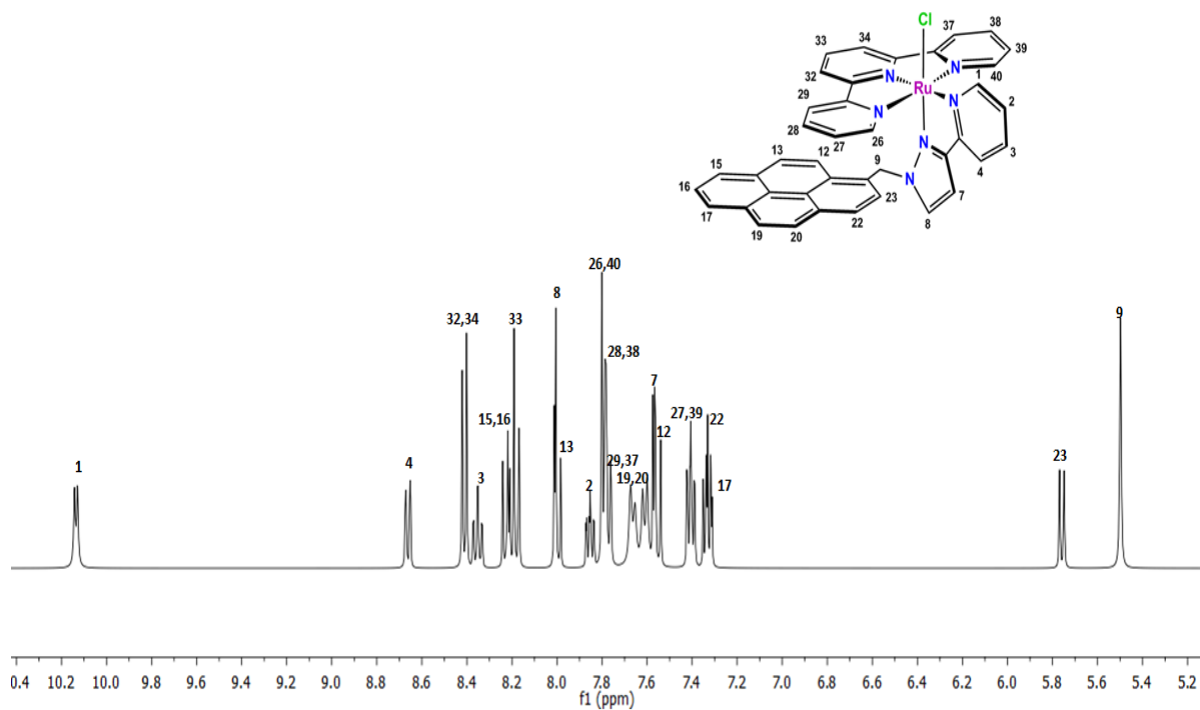**Figure 8**. ^{13}C-NMR spectra corresponding to the ligand **L3**

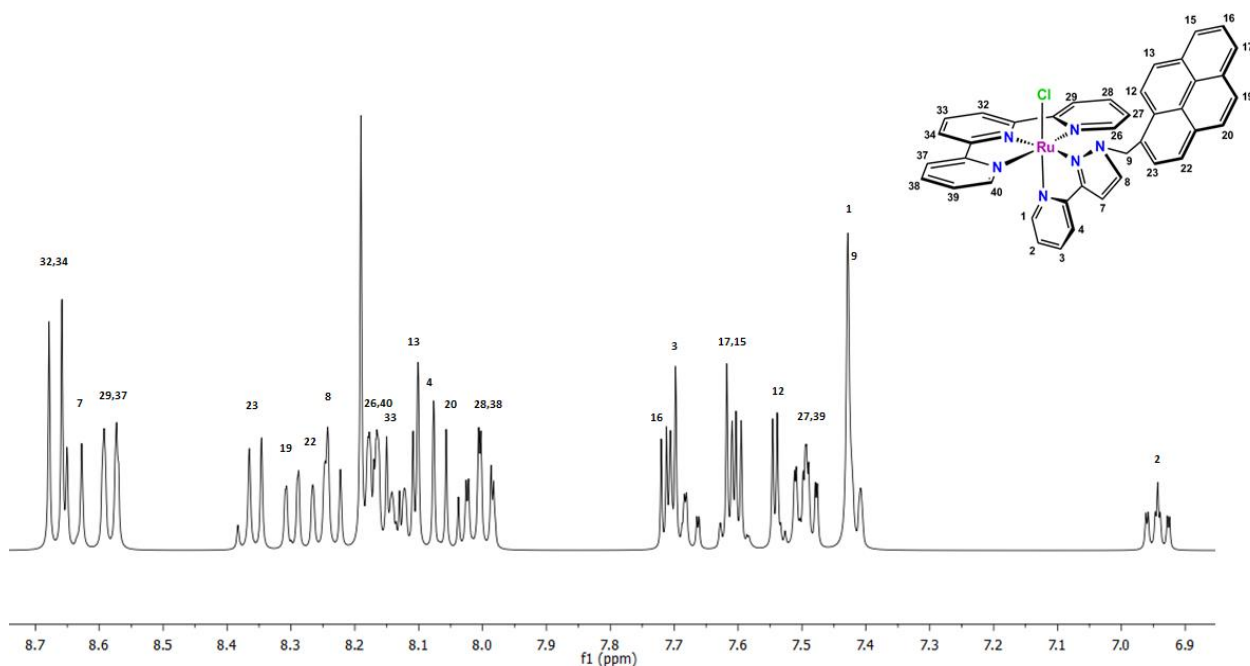**Figure 9**. ^{1}H-NMR spectrum corresponding to the trans **C2a**

Figure 10. ^{1}H-NMR spectra corresponding to the cis **C2b**

4.2.3 UV-visible spectroscopy

The UV-Vis spectra for all complexes registered in CH_2Cl_2 or aqueous phosphate buffer are displayed in Figure 11. The complexes exhibit ligand based π-π* bands below 350 nm and relatively intense bands above 330 nm mainly due to $d\pi(Ru)$-π*(L) MLCT transitions.[24] It is worth noting that the presence of an alkyl pyrene substituent at the pyrazole ring induces a hypsochromic shift of the MLCT absorptions with regard to the analogous complex bearing the unsubstituted pypz-H ligand, which is in accordance with a decrease of the electron density donation from the pypz-pyrene ligand to the metal. For the Ru-OH_2 complexes the MLCT bands are shifted to the blue with regard to the corresponding Ru-Cl complexes due to the higher stabilization of the $d\pi$ (Ru) levels provoked by the OH_2 ligand in comparison with the Cl one.
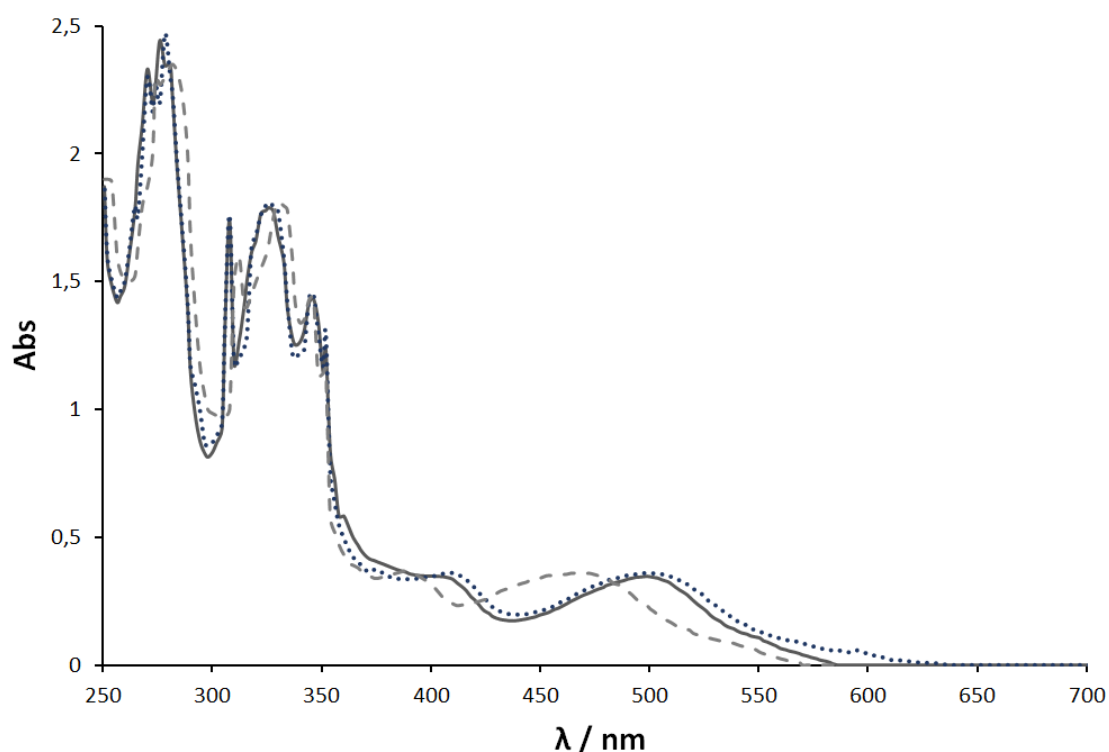
19

Figure 11. UV/Vis spectra of **C2a** (solid black line), **C2b** (dotted blue line) in CH_2Cl_2 and **C3a** (dashed grey line) in phosphate buffer (pH=6.8)

4.3 Electrochemical properties

The redox properties of the ligand pypz-pyrene and compounds have been determined by cyclic voltammetry (CV) experiments and differential pulse voltammetry (DPV) in CH_2Cl_2 + 0.1 M TBAP or phosphate buffer (pH=6.8), using glassy carbon electrodes as working electrodes and are displayed in Figures 12-14 and 17. Ligand pypz-pyrene displays a one irreversible peak at 1.4 V vs SCE that can be attributed to the electro-oxidation of the pyrene monomer to its cationic radical (Figure 12).[25] Chlorido complexes *trans*-**C2a** and *cis*-**C2b** exhibit reversible monoelectronic Ru(III/II) redox waves at around $E_{1/2}$ = 0.85 and 0.88 V vs. SCE respectively, and one irreversible peak at 1.4 V that corresponds to the oxidation of the pyrene monomer to its cation radical (Figure 13-14). For the aquo *trans*-**C3a**, two quasireversible processes are observed at $E_{1/2}$ = 0.43 and 0. 62 V vs. SCE at pH=6.8 that correspond to Ru(III/II) and Ru(IV/III) redox couples, respectively (Figure 17).
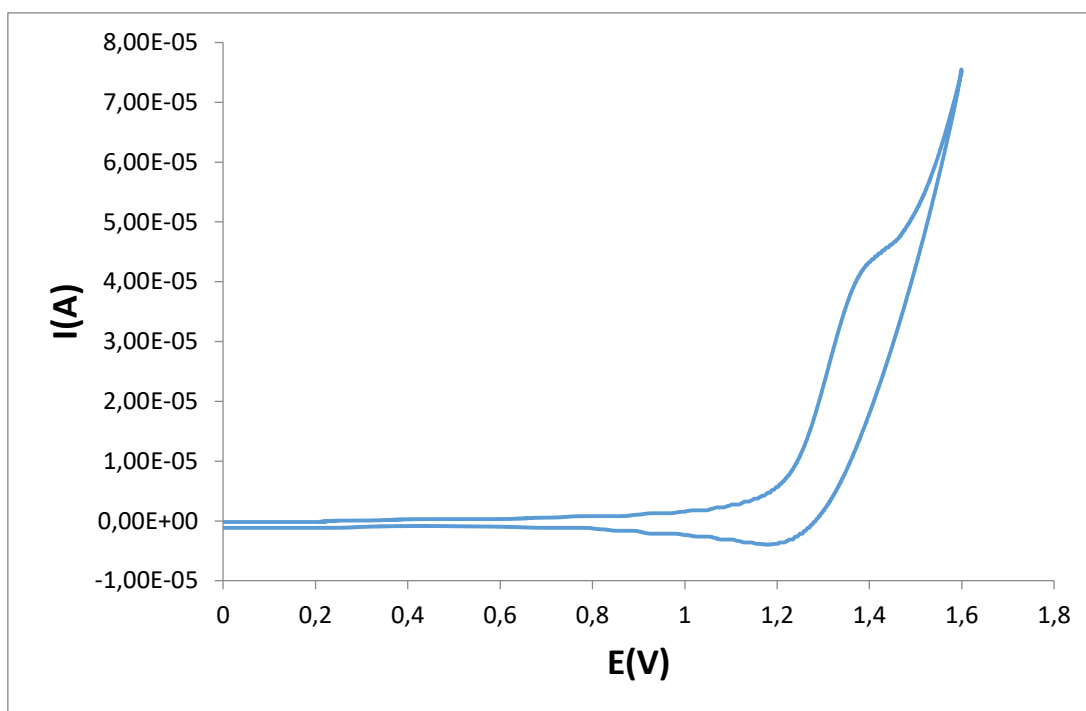
20

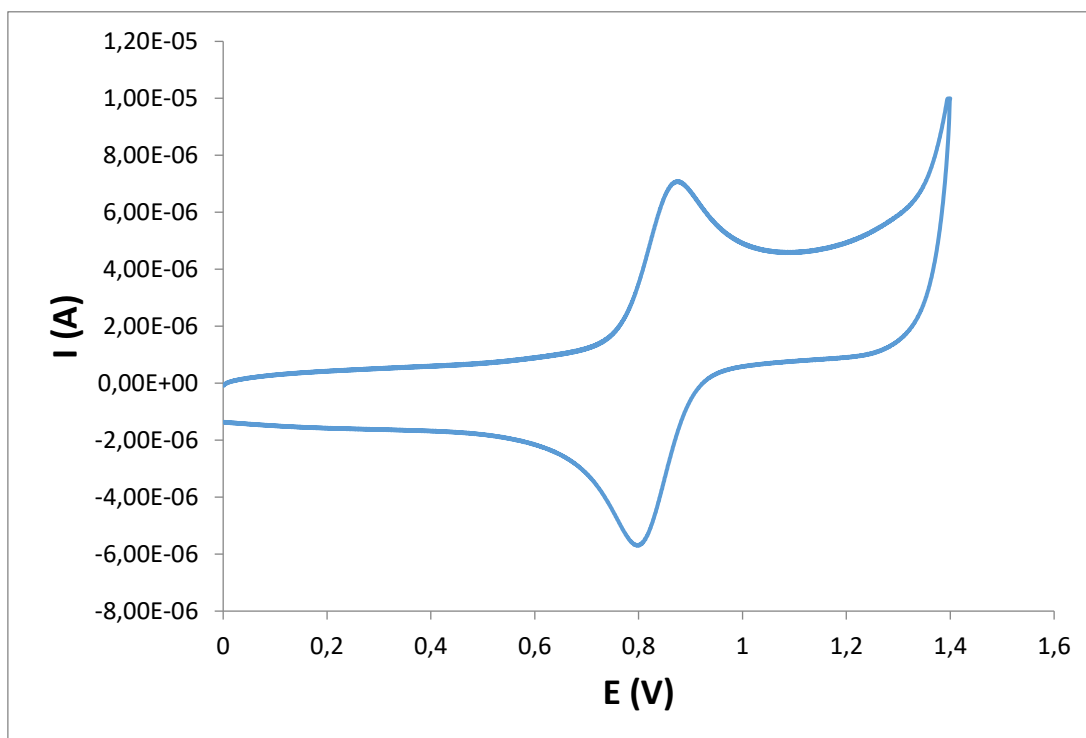**Figure 12**. CV for the ligand **L3** in CH_2Cl_2 + 0.1 M TBAP

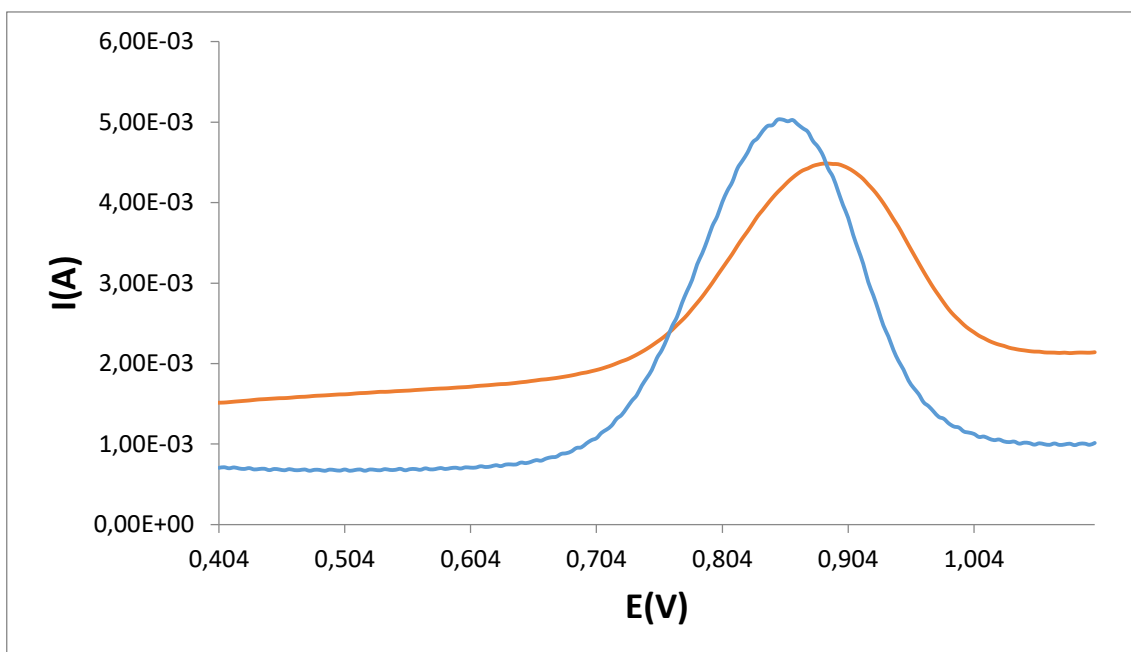**Figure 13**. CV for chloro complex **C2a** (trans) in CH_2Cl_2 + 0.1 M TBAP

Figure 14. DPV for complex **C2a** (blue) and **C2b** (orange) in CH_2Cl_2 + 0.1 M TBAP

For chlorido and aqua complexes, upon repetitive oxidative scanning between 0 and 1.6 V for **C2a** and 0 and 1.2 for **C3a**, leads to the electropolymerization of pyrene compounds onto the electrode surface that is observed by the increase in the intensity of the oxidation peaks (Figures 15 and 17, respectively). After oxidation of the pyrene group into its cationic radical, this initiates the polymerization process via coupling of pyrene radicals. After the polymerization process and upon transfer into a new solution of CH_2Cl_2 + 0.1 M TBAP or phosphate buffer, we can observe the signals correspond to the monoelectronic Ru(III/II) redox wave for **C2a** and the two redox processes Ru(III/II) and Ru(IV/III) for the aqua complex **C3a** (Figures 16 and 18, respectively).
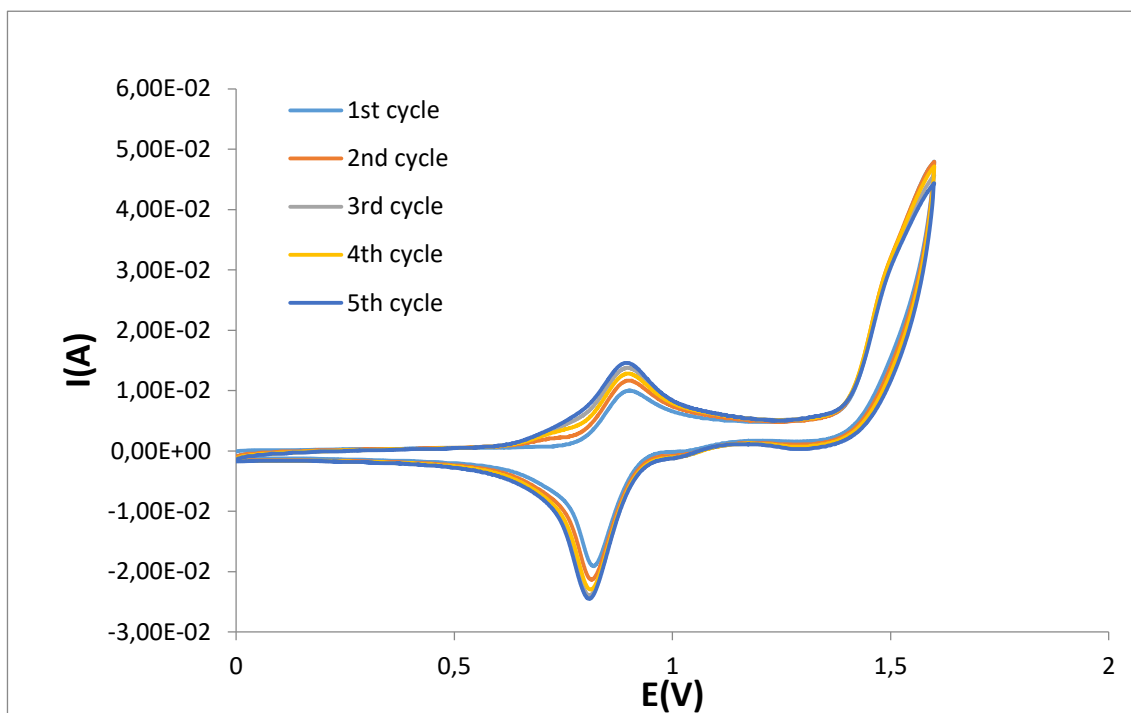
Figure 15. Polymerization of compound **C2a** onto a glassy carbon electrode in CH_2Cl_2
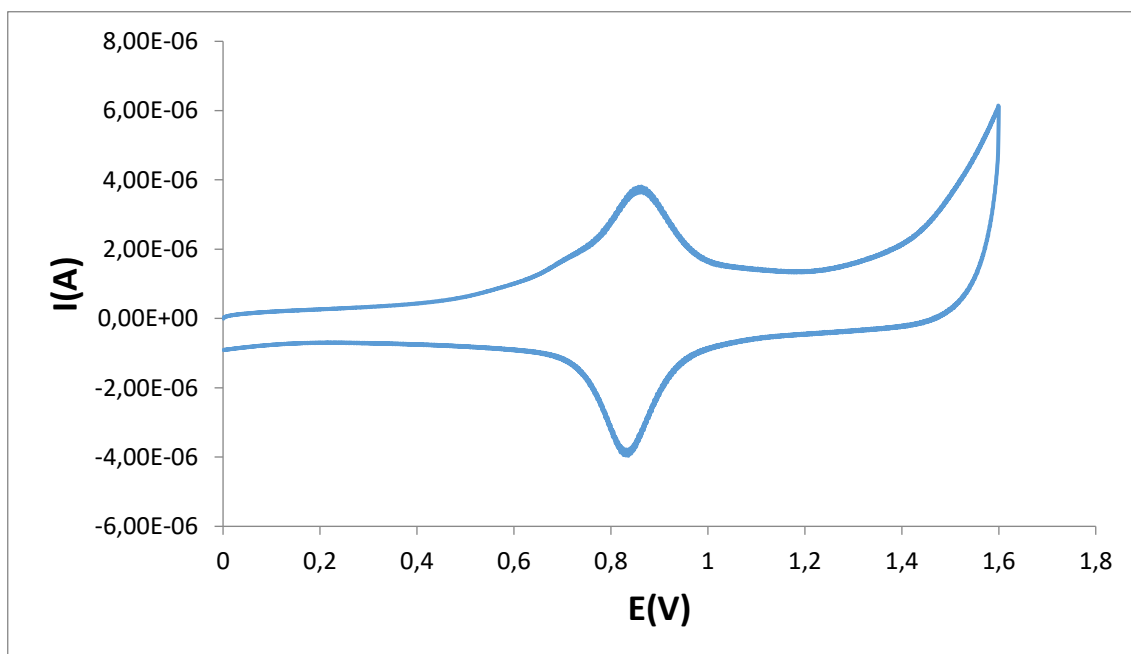+ 0.1 M TBAP

Figure 16. CV of the polymer film generated Poly-**C2a** in CH_2Cl_2 + 0.1 M TBAP
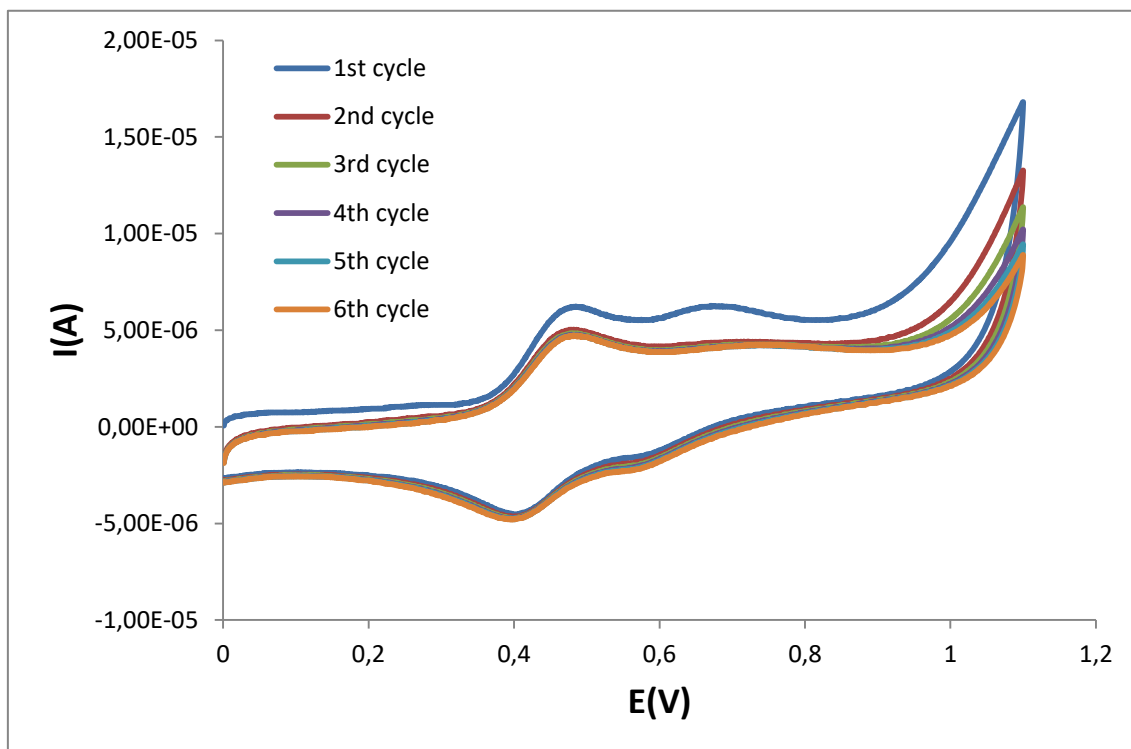
Figure 17. Polymerization of compound **C3a** onto a glassy carbon electrode in phosphate buffer.
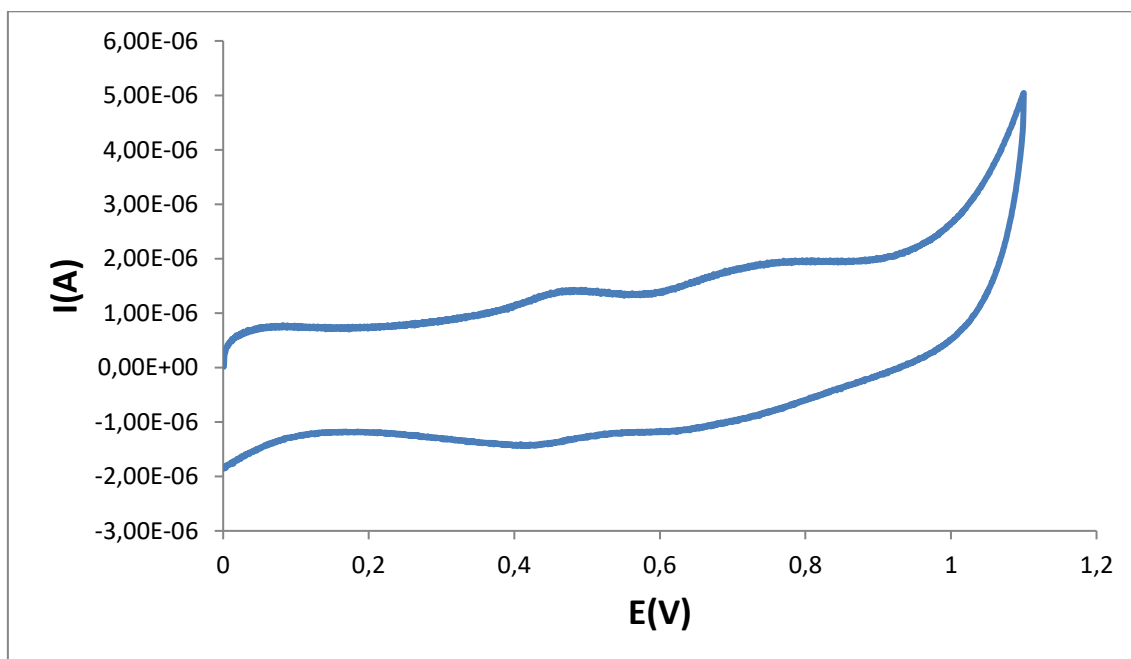

Figure 18. CV of the polymer film generated Poly-**C3a** in phosphate buffer.

The redox potentials for the Ru-aqua complexes are pH dependent due to the capacity of the mentioned aqua ligand to lose protons as has been shown in the introduction.

The complete thermodynamic information regarding the Ru-aqua complex can be extracted from the Pourbaix diagrams, exhibited in Figure 19 for **C3a**. There, the relation between the potential and the pH is given through Equation 1

$$E_{1/2} = E°_{1/2} - 0.059 \ (m/n) \ pH \tag{1}$$

$E_{1/2:}$ half wave redox potential at a given pH
$E°_{1/2:}$ half wave redox potential at standard conditions
m: number of transferred protons
n: number of transferred electrons

Equation 1. Relation between potential and pH in the Nernst equation.
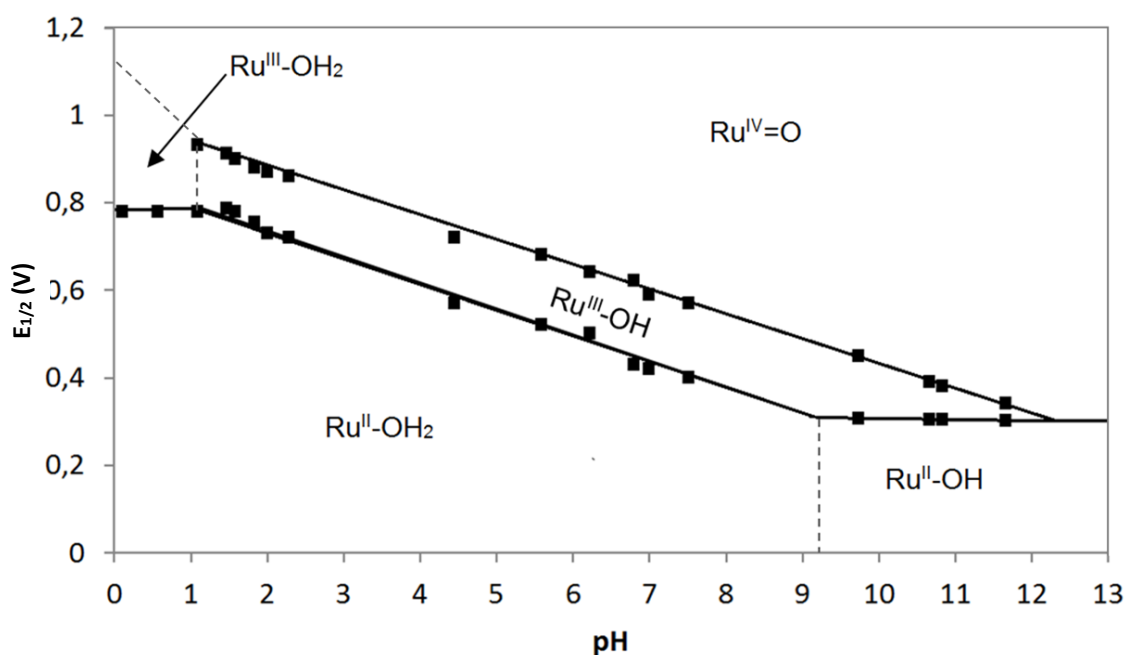

Figure 19. Pourbaix diagram for complex **C3a**. The stability zones and the proton composition for the different redox species are indicated. The pKa of each species are represented with dashed vertical lines.

At pH values around 1.1 and 9.3, the medium wave potential is sensitive to the pH of the solution and decreases linearly with the increase of pH with a slope of 60 mV per unit of pH. This value is very close to the theoretical value of the Nernst equation for process in which one electron and one proton are lost. The process taking place on this pH it is indicated on the following equation (2):

$$[Ru^{II}(trpy)(pypz\text{-}pyrene)(OH_2)]^{2+} \;\rightleftharpoons\; [Ru^{III}(trpy)(pypz\text{-}pyrene)(OH)]^{+} + 1H^{+} + e^{-} \quad (2)$$

On this same range of pH, it is seen another redox process corresponding to the second ruthenium oxidation, from Ru(III) to Ru(IV). For this second process, the potential decreases with a slope of 55mV per unit of pH. Again, this value is very close to the one in the Nernst equations, so in this process one electron and one proton are lost. This process it is represented by the following equation (3):
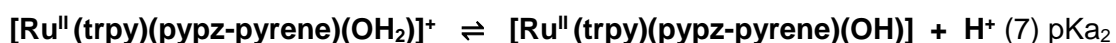
$$[Ru^{III}(trpy)(pypz\text{-}pyrene)(OH)]^{+} \;\rightleftharpoons\; [Ru^{IV}(trpy)(pypz\text{-}pyrene)(O)]^{+} + 1H^{+} + e^{-} \quad (3)$$

Under acid conditions, pH < 1.1, the medium wave potential is pH independent ($E_{1/2}$ = 0.78 V) and the process can be represented with the following equation (4):

$$[Ru^{II}(trpy)(pypz\text{-}pyrene)(OH_2)]^{+} \;\rightleftharpoons\; [Ru^{III}(trpy)(pypz\text{-}pyrene)(OH_2)]^{2+} + e^{-} \quad (4)$$

On the other hand, under basic conditions, pH > 9.3, the medium wave potential is pH independent as well ($E_{1/2}$ = 0.30 V) and the process can be represented with the following equation (5):

$$[Ru^{II}(trpy)(pypz\text{-}pyrene)(OH)] \;\rightleftharpoons\; [Ru^{III}(trpy)(pypz\text{-}pyrene)(OH)]^{+} + e^{-} \quad (5)$$

The dashed vertical lines indicate the pka. The first one corresponds to the pKa_1 (1.10), the second is the pka_2 (9.32). They also correspond to the acid-base equilibrium of the $Ru^{III}\text{-}OH_2$ and $Ru^{II}\text{-}OH_2$ species, respectively. They are indicated in the following equations (6) and (7):

$$[Ru^{III}(trpy)(pypz\text{-}pyrene)(OH_2)]^{2+} \;\rightleftharpoons\; [Ru^{III}(trpy)(pypz\text{-}pyrene)(OH)]^{+} + H^{+} \quad (6)\ pKa_1$$

$$[Ru^{II}(trpy)(pypz\text{-}pyrene)(OH_2)]^{+} \;\rightleftharpoons\; [Ru^{II}(trpy)(pypz\text{-}pyrene)(OH)] + H^{+} \quad (7)\ pKa_2$$
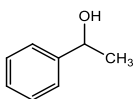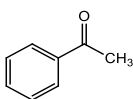
4.4 Catalytic experiments

The photocatalytic oxidation of 1-phenyl ethanol was performed in 3 ml of phosphate buffer pH 6.8 under irradiation with a xenon lamp (150, Hamamatsu LC8), equipped with a 400-700 nm large band filter. The system contains: 0.5 mM of **C3a** as catalyst, 5 mM of photosensitizer $[Ru(bpy)_3]Cl_2$, 50 mM of alcohol substrate and 100 mM of oxidizing agent sodium persulfate ($Na_2S_2O_8$). Then, following irradiation for 15 h, the reaction products were extracted with dichloromethane three times, dried with Na_2SO_4 and evaluated by means of ^{1}H-NMR spectroscopy. The selectivity obtained was >99%.

Also, the conversion yield appears on the following table

Table 4. Ru-catalyzed alcohol oxidation

Substrate	Product	Yield (%)
		52

A proposed photocatalytic cycle for the oxidation of 1-phenyl ethanol is shown in scheme 4.
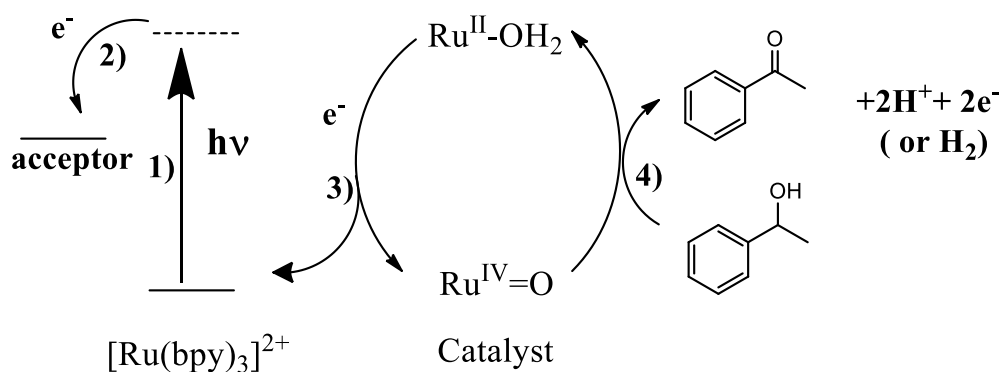
Scheme 4. Steps involving photooxidation process

CHAPTER 5. CONCLUSIONS

1. A new ligand, the 3-(2-pyridyl)-1-(pyrazolyl)methylpyrene, (pypz-pyrene, **L3**) and new ruthenium complexes containing the tridentate trpy and the no symmetric bidentate pypz-pyrene ligands, *trans* and *cis*-[RuCl(trpy)(pypz-pyrene)](PF_6) **C2a** and **C2b** and *trans*-[Ru(trpy)(pypz-pyrene)(OH_2)](PF_6)$_2$ **C3a**, have been synthesized and thoroughly characterized by structural, analytical, spectroscopic and electrochemical techniques.

2. In the case of the chlorido complex, a mixture of two isomers (*trans* and *cis*) were obtained in a 1:0.5 ratio and, were separated by column chromatography. The formation of higher amount of isomer *trans*, could be explained on the basis of electronic effects, as we have evidenced in similar structural complexes described in the literature. The crystal structure of both isomers has been solved through X-ray diffraction analysis, showing a distorted octahedral environment for the Ru metal centre.

3. The aqua-complex **C3a** was obtained after refluxing the chlorido complex **C2a** in a mixture of H_2O/acetone (2:1) in the presence of Ag^+ as precipitating reagent.

4. The spectroscopic NMR analysis are consistent with the presence of the corresponding compounds in solution.   In the case of **C2a** complex a strong downfield shift is observed for the pyridylic proton located next to the chlorido ligand; this proton appears a highfield shift in the case of isomer **C2b**.

5. The redox characterization of ligand pypr-pyrene displays a one irreversible peak at 1.4 V vs SCE, that can be attributed to the electro-oxidation of the pyrene monomer to its cationic radical. Chlorido complexes *trans*-**C2a** and *cis* -**C2b** exhibit reversible monoelectronic Ru(III/II) redox waves at around $E_{1/2} =$ 0.85 and 0.88 V vs. SCE respectively, and one irreversible peak at 1.4 V that corresponds to the oxidation of the pyrene substituent.

6. **C3a** complex displays two pH-dependent redox processes corresponding to the Ru^{IV}/Ru^{III} and Ru^{III}/Ru^{II} redox pairs. The Pourbaix diagram indicates that two deprotonation processes can take place, corresponding to the deprotonation of aqua ligand.

7. Electropolymerization of the complexes onto glassy carbon electrodes was carried out, upon repetitive oxidative scanning between 0 and 1.6 V for **C2a** and 0 and 1.2 for **C3a**. This electropolymerization of pyrene compounds is observed by the increase in the intensity of the oxidation peaks.

8. Compound **C3a** was tested in the oxidation of 1-phenyl alcohol in waterl, showing moderate conversion and high selectivity values.

CHAPTER 6. BIBLIOGRAPHY

[1] Qu, P.; Thompson, D. W.; Meyer, G. J. *Langmuir,* **2000**, *16*, 4662.

[2] (a) Murahashi, S.I.; Takaya, H.; Naota, T. *Pure Appl. Chem.* **2002**, *74*, 19. (b) Rodríguez M.; Romero, I.; Llobet, A.; Deronzier, A.; Biner, M.; Parella, T.; StoeckliEvans H. *Inorg. Chem.* **2001**, *40*, 4150.

[3] (a) Nikolau, S.; Toma, H.E. *J. Chem. Soc., Dalton Trans.* **2002**, 352. (b) Rodríguez, M.; Romero, I.; Llobet, A.; Collomb-Dunand-Sauthier, M. N.; Deronzier, A.; Parella, T.; Stoeckli-Evans, H. *J. Chem. Soc., Dalton Trans.* **2000**, 1689.

[4] Clarke, M. J. *Coord. Chem. Rev.* **2003**, *236*, 209.

[5] Balzani, V.; Bergamini, G.; Marchioni, F.; Ceroni, P. *Coord. Chem. Rev.* **2006**, *250*, 1254.

[6] Zhang, S.; Ding, Y.; Wei, H. *Molecules* **2014**, *19*, 11933.

[7] Coe, B. J. *Coord. Chem. Rev.* **2013**, *257*, 1438. (b) Yoshida, J.; Watanabe, G.; Kakizawa, K.; Kawabata, Y.; Yuge, H. *Inorg. Chem.* **2014**, *52*, 11042.

[8] Zhang, S.; Ding, Y.; Wei, H. *Molecules* **2014**, *19*, 11933.

[9] (a) Serrano, I.; López, M. I.; Ferrer, I.; Poater, A.;Parella, T. ; Fontrodona, X.; Solà, M.; Llobet, A.; Rodríguez, M.; Romero, I. *Inorg. Chem.* **2011,** *50,* 6044. (b) Dakkach, M.;Fontrodona, X.; Parella, T.; Atlamsani, A.; Romero, I.; Rodríguez, M. *Adv. Synth. & Catal..* **2011,** *353*, 231.

[10] (a) Alstreen-Acebedo, J. H.; Brennaman, M.K.; Meyer T.U. *Inorg. Chem.* **2005**, *44*, 6802. (b) Hammarstrom, L.; Sun, L.C.; Akermark, B.; Stryring, S. *Catal. Today.* **2000**, *58*, 57.

[11] (a) Barigelletti, F.; Flamigni, L. *Chem. Soc. Rev.* **2000**, *29*, 1. (b) Yin, J.-F.; Velayudham, M.; Bhattacharya, D.; Lin, H.-C.; Lu, K.-L. *Coord. Chem. Rev.* **2012**, *256*, 3008.

[12] Jiang, C.W.; Chao, H.; Hong, X. L.; Li, H.; Mei, W. J.; Ji, L. N. *Inorg. Chem. Commun.* **2003**, *6*, 773.

[13] Costentin, C.; Robert, M.; Saveant, J.-M. *Chem. Rev.* **2010**, *110*, PR1-PR40.

[14] Young, E. R.; Costi, R.; Paydavosi, S.; Nocera, D. G.; Bulovic, V. *Energy Environ. Sci.* **2011**, *4*, 2058.

[15] Blakemore, D.; Crabtree, J. H.;Brudvig, R. W. (**2015**). *Molecular Catalysts for Water Oxidation*. New Haven, Connecticut: ACS Publications, pp.12974-12980.

[16] (a) Ko, S. Y.; Lee, A. W. M.; Masamune, S. ; Reed, L. A. ; Sharpless, K. B.; Walker F. J. *Science* **1983**, *220*,949.(b) Nicolaou, K.C.; Winssinger, N.; Pastor, J .; Ninkovic, S.; Sarabia, F.; He, Y.; Vourloumis, D.; Yang, Z.; Li, T. ; Giannakakou, P.; Hamel, E. *Nature* **1997**, *387*, 268; (c) Gagnon S.D. in Encyclopedia of Polymer Science Engineering, 2nd ed. (Eds: Mark, H.F.; Bikales, N. M.;. Overberger, C. G; Menges G.; Kroschwitz J. I.) Wiley-VCH, Weinheim, **1994**,p p. 275–307; (d) Darensbourg, D.J.; Mackiewicz, R. M.; Phelps, A. L.; Billodeaux, D. R. *Acc. Chem. Res.* **2004**, *37*, 836;(e) Jacobsen, E.N.Catalytic Asymmetric Synthesis (Ed:I.Ojima), VCH, New York, **1993**, p.229;(f) DeFaveri, G.; Ilyashenko, G. ; Watkinson, M. *Chem. Soc. Rev.* **2011**, *40*,1722.

[17] Crabtree, R. H. Energy Production and Storage – Inorganic Chemical Strategies for a Warming World, Encyclopedia of Inorganic Chemistry, ed., John Wiley & Sons, Inc., 2nd ed, **2010**, pp. 73–87.

[18] Ferrer, I.; Fontrodona, X.; Roig, A.; Rodríguez, M. Romero, I.; *Chem. Eur. J.* **2017**, *23*, 4096.

[19] Esswein, A. J. ; Nocera, D. G. *Chem. Rev.* **2007**, *107*, 4022.

[20] (a) Chen, W.; Rein F. N.; Rocha, R. C. *Angew. Chem., Int. Ed.,* **2009**, *48*, 9672; (b) Chen, W. ; Rein, F. N.; Scott B. L. ;Rocha, R. C. *Chem. Eur. J.,* **2011**, *17*, 5595. (c) Li, F. ; Yu, M. ; Jiang, Y.; Huang, F. ; Li, Y.; Zhang B. ; Sun, L. *Chem. Commun.,* **2011**, 47, 8949.

[21] Brunner, H.; Scheck, T. *Chem. Ber.* **1992**, *124*,701.

[22] Sullivan, B. P.; Calvert, M.; Meyer, T. J. *Inorg. Chem.* **1980**, *19*, 1404.

[23] (a) Manrique, E.;Fontrodona, X.; Rodriguez, M.; Romero, I. *Eur. J. Inorg. Chem.* **2019**, 2124. (b) Dakkach, M.; López, M. I.; Romero, I.; Rodríguez, M.; Atlamsani, A.; Parella, T.; Fontrodona, X.; Llobet, A. *Inorg. Chem.* **2010**, *49*, 7072.

[24] Balzani, V.; Juris, A.; Venturi, M.; Campagna, S.; Serroni, S. *Chem. Rev.* **1996**, *96*, 759.

[25] Waltman R.J.; Diaz, A.F.; Bargon, J. *Electrochem. Soc.***1985**, *132,* 631.